

AD-A145 624

SOLVENT EFFECTS UPON ELECTROCHEMICAL KINETICS:
INFLUENCES OF INTERFACIAL... (U) PURDUE UNIV LAFAYETTE IN
DEPT OF CHEMISTRY M J WEAVER SEP 84 TR-38

1/1

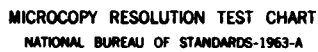
UNCLASSIFIED

N00014-79-C-0670

F/G 7/4

NL





MICROCOPY RESOLUTION TEST CHART
NATIONAL BUREAU OF STANDARDS-1963-A

AD-A145 624

DTIC FILE COPY

OFFICE OF NAVAL RESEARCH
Contract N00014-79-C-0670

(2)

TECHNICAL REPORT NO. 38

Solvent Effects upon Electrochemical Kinetics:

Influences of Interfacial Solvation and

Solvent Relaxation Dynamics

by

M. J. Weaver

Prepared for Publication

in the

"Proc. NATO Advanced Study Institute on

Trends in Interfacial Electrochemistry

Department of Chemistry

Purdue University

West Lafayette, IN 47907

September 1984

DTIC
SELECTED
SEP 19 1984
A

Reproduction in whole or in part is permitted for
any purpose of the United States Government

This document has been approved for public release
and sale; its distribution is unlimited

84 09 18 301

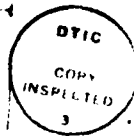
REPORT DOCUMENTATION PAGE		READ INSTRUCTIONS BEFORE COMPLETING FORM
1. REPORT NUMBER	2. GOVT ACCESSION NO.	3. RECIPIENT'S CATALOG NUMBER
Technical Report No. 38		
4. TITLE (and Subtitle) Solvent Effects upon Electrochemical Kinetics: Influences of Interfacial Solvation and Solvent Relaxation Dynamics		5. TYPE OF REPORT & PERIOD COVERED Technical Report No. 37
		6. PERFORMING ORG. REPORT NUMBER
7. AUTHOR(s) M. J. Weaver		8. CONTRACT OR GRANT NUMBER(s) N00014-79-C-0670
9. PERFORMING ORGANIZATION NAME AND ADDRESS Department of Chemistry Purdue University West Lafayette, IN 47907		10. PROGRAM ELEMENT, PROJECT, TASK AREA & WORK UNIT NUMBERS
11. CONTROLLING OFFICE NAME AND ADDRESS Office of Naval Research Department of the Navy Arlington, VA 22217		12. REPORT DATE September 1984
		13. NUMBER OF PAGES
14. MONITORING AGENCY NAME & ADDRESS (if different from Controlling Office)		15. SECURITY CLASS. (of this report) Unclassified
		15a. DECLASSIFICATION/DOWNGRADING SCHEDULE
16. DISTRIBUTION STATEMENT (of this Report) Approved for Public Release; Distribution unlimited		
17. DISTRIBUTION STATEMENT (of the abstract entered in Block 20, if different from Report)		
18. SUPPLEMENTARY NOTES		
19. KEY WORDS (Continue on reverse side if necessary and identify by block number) inorganic and organometallic complexes; inner-shell barrier; electrochemical kinetics		
20. ABSTRACT (Continue on reverse side if necessary and identify by block number) Some likely influences of the solvent medium upon the kinetics of simple electrochemical reactions are described, and illustrated with recent results from the author's laboratory.		

DD FORM 1473

NTIS GRA&I
DTIC TAB
Unannounced
Justification

By
Distribution/
Availability Codes

Avail. and/or
Spec. and



SOLVENT EFFECTS UPON ELECTROCHEMICAL KINETICS: INFLUENCES OF
INTERFACIAL SOLVATION AND SOLVENT RELAXATION DYNAMICS

Michael J. Weaver
Department of Chemistry, Purdue University
West Lafayette, Indiana 47907, U.S.A.

Some likely influences of the solvent medium upon the kinetics of simple electrochemical reactions are described, and illustrated with recent results from the author's laboratory.

Introduction

The solvent has long been known to exert profound influences on the kinetics of electron-transfer reactions at electrode surfaces as well as in homogeneous solution. Nevertheless, our understanding of such solvent effects has remained demonstrably inadequate. This is undoubtedly due in large part to the frequency manifold origins of the effects observed upon variation of the solvent medium, arising in part from alterations in the chemical nature of the reactant as well as from longer-range reactant-solvent interactions.

A valuable class of model systems is provided by one-electron couples involving substitutionally inert inorganic and organometallic complexes. Important virtues of these systems include the opportunity to hold constant the free-energy barrier associated with metal-ligand vibrations ("inner-shell" barrier) as the solvent is altered, along with the ability to vary the nature of the reactant-solvent interactions by means of alterations in the ligand structure as well as the solvent.

~~The present conference~~ ^{> This} paper is intended as a summary of some recent research in our laboratory aimed at gaining a fundamental understanding of solvent effects in electrochemical kinetics. Besides examining the effects of altering the bulk solvent, experiments are also described where the influence of

From S. R. → the interfacial solvent structure in aqueous media is probed through variations in the hydrophilicity of the metal surface. Particularly since some of this recent experimental activity has been associated closely with concurrent theoretical development, it is useful at the outset to provide a brief summary of the underlying kinetic formulations. ←

I. Fundamental Rate Expressions

The observed rate constant for outer-sphere electron transfer, k_{ob} , can be related to the corresponding activation free energy for the elementary electron-transfer step, ΔG^* , by (1)

$$k_{ob} = K_p \nu_n \kappa_{el} \Gamma_n \exp(-\Delta G^*/RT) \quad \text{Eq. 1}$$

where K_p (cm) is the effective equilibrium constant for forming the "precursor state" in the double layer from the bulk reactant, ν_n (sec^{-1}) is the nuclear frequency factor, κ_{el} is the electron-tunneling probability in the transition state, and Γ_n is the nuclear-tunneling factor. (The last term is close to unity for most reactions.) This relation is based on an "encounter preequilibrium" formulation of the preexponential factor, rather than the more conventional collisional model. The fundamental correctness of the former for electrochemical processes has been emphasised (1). It envisages electron transfer taking place via unimolecular activation of reactant in sufficiently close proximity to the electrode surface so that the electron-tunneling probability, κ_{el} , is suitably large. Since κ_{el} decreases sharply as the reactant-electrode distance increases, the inevitable integral of reaction sites will contain dominant contributions from those involving close approach of the reactant to the metal surface (2). For so-called "nonadiabatic pathways", $\kappa_{el} \ll 1$ even at the plane of closest approach, whereas for "adiabatic pathways" $\kappa_{el} \sim 1$ under these conditions. By analogy with homogeneous electron-transfer processes, heterogeneous outer-sphere pathways can be regarded as those where the reactant does not penetrate the inner layer ("coordination layer") of solvent molecules immediately adjacent to the metal surface. However, as discussed below the kinetics of such reactions may nonetheless be influenced significantly by the interfacial solvent environment.

The nature of solvent medium can yield important influences on several of these terms. These will now be considered in turn.

(i) *Precursor stability constant, K_p .* This quantity can be expressed for electrochemical reactions as

$$K_p = K_o \exp(-w_p/RT) \quad \text{Eq. 2}$$

where w_p is the work of transporting the reactant from the bulk solution to the predominant reaction site, and K_o (cm) is a statistical term. The latter is numerically equal to the effective "reaction zone thickness", within which the reactant needs to be located in order to contribute importantly to the overall reaction rate (2). For nonadiabatic or weakly adiabatic reactions, $K_o \sim 0.5$ to 2 \AA (2).

For *bona fide* outer-sphere reactions, it is convenient to express Eq. 1 instead in terms of the conventional "double-layer corrected" rate constant, k_{corr} :

$$k_{\text{corr}} = K_o v_n \kappa_{el} \Gamma_n \exp(-\Delta G_{\text{corr}}^*/RT) \quad \text{Eq. 3}$$

where ΔG_{corr}^* is a work-corrected free energy of activation. Both k_{corr} and ΔG_{corr}^* are the quantities that would be observed in the absence of coulombic double-layer effects; k_{corr} is related to k_{ob} on the basis of the simple Frumkin model by (3)

$$\ln k_{\text{corr}} = \ln k_{\text{ob}} + (Z_r - \alpha_{\text{corr}}) \phi_r F/RT \quad \text{Eq. 4}$$

where Z_r is the charge number of the oxidized form of the redox couple, α_{corr} is the work-corrected cathodic transfer coefficient, and ϕ_r is the average potential at the reaction site with respect to the bulk solution. Equation 4 can be related to Eqs. 1 - 3 if it is assumed that $w_p = ZF\phi_r$ and $\Delta G^* = \Delta G_{\text{corr}}^* + \alpha_{\text{corr}} F\phi_r$.

Besides the niceties of discreteness-of-charge effects, additional contributions to w_p might be envisaged if the solvating environment in the vicinity of the reaction site in the double layer differs from that in the bulk solution. Such a "specific" work term contribution will occur if the reactant is partly desolvated in the transition state. This is considered briefly in Section II. This circumstance may apply even for outer-sphere reactions at interfaces where the local solvent structure is strongly perturbed by the metal surface (Section III).

(ii) *Electron Tunneling Probability, κ_{el}* . Although the probability of electron tunneling for outer-sphere systems is anticipated to be relatively insensitive to the intervening medium (4), the nature of the solvent may affect κ_{el} through its influence upon the reactant-electrode distance, x . This is because the reactant in the outer-sphere transition state is expected to be separated from the metal surface by a layer of

solvent molecules. Therefore the size of the solvent molecules, together with their ability to solvate the reacting species, should influence κ and hence κ_{el} .

(iii) *Nuclear Frequency Factor, ν_n* . This quantity denotes the effective frequency with which the reacting system surmounts the free-energy barrier. The magnitude of ν_n will be determined both by the characteristic inner-shell (reactant vibration) and outer-shell (solvent polarization) frequencies, ν_{is} and ν_{os} respectively, appropriately weighted according to the corresponding inner- and outer-shell components of ΔG^*_{corr} ; ΔG^*_{is} , ΔG^*_{os} , respectively. When $\Delta G^*_{is} \rightarrow 0$, $\nu_n = \nu_{os}$, whereas when $\Delta G^*_{is} \sim \Delta G^*_{os}$, $\nu_n = \nu_{is}$ (1). The solvent dynamics should therefore influence the preexponential factor for reactions where the inner-shell barrier is small. This question is considered in Section III.

(iv) *Free-energy barrier, ΔG^** . The influence of the surrounding solvent, as well as other environmental influences upon ΔG^*_{corr} , is conventionally divided into so-called "intrinsic" and "thermodynamic" (or "extrinsic") contributions (5,6). The latter is identified with the solvent influence upon the standard (or "formal") potential E_f of the redox couple, and hence upon the thermodynamic driving force at a given electrode potential E , whereas the latter is associated with the solvent contribution to the free-energy barrier when the driving force is zero, i.e., when $E = E_f$. For electrochemical reactions involving multi-electron transfer and/or coupled chemical steps, these contributions cannot be separated entirely since E_f for the required rate-determining electron-transfer step (as opposed to the overall reaction) will be unknown.

We shall consider here the influence of the solvent upon the intrinsic barrier, $\Delta G^*(int)$. The work-corrected standard rate constant, k^s_{corr} , (i.e., that measured at E_f) can be related to $\Delta G^*(int)$ by [c.f. Eq. 3]:

$$k^s_{corr} = K_o \nu_n \kappa_{el} \Gamma_n \exp[-\Delta G^*(int)/RT] \quad \text{Eq. 5a}$$

$$\text{where } \Delta G^*(int) = \Delta G^*_{os}(int) + \Delta G^*_{is}(int) \quad \text{Eq. 5b}$$

The inner-shell contribution to $\Delta G^*(int)$, $\Delta G^*_{is}(int)$, will remain essentially constant in different solvents providing that the coordination sphere remains unchanged. The solvent contribution to $\Delta G^*(int)$, $\Delta G^*_{os}(int)$, for electrochemical reactions can be estimated on the basis of the conventional dielectric continuum treatment from (7)

$$\Delta G^*_{os}(int) = \frac{e^2}{8} \left(\frac{1}{a} - \frac{1}{R} \right) \left(\frac{1}{\epsilon_{op}} - \frac{1}{\epsilon_s} \right) \quad \text{Eq. 6}$$

where e is the electronic charge, a is the reactant radius, R is twice the reactant-electrode distance, and ϵ_{op} and ϵ_s are the optical and static dielectric constants, respectively (7). While the quantitative, or even qualitative, validity of the dielectric continuum treatment has been questioned (8), it has proved relatively successful in predicting the energetics of photo-induced electron transfer in homogeneous intramolecular systems, for which the barrier height can be extracted directly from spectral data (9). The approximate success of Eq. 6 is probably associated with the dominance of the ϵ_{op} term, since typically $\epsilon_{op} \ll \epsilon_s$. Thus although the "static" component of the barrier (the ϵ_s term) is liable to be seriously in error for many systems as a consequence of dielectric saturation, etc., the "optical" component (associated with ϵ_{op}) is anticipated to be relatively insensitive to the local solvent structure. The errors in the "static" component in Eq. 6 have been estimated to be no greater than 1 - 1.5 kcal mol⁻¹ even for systems displaying strong specific ligand-solvent interactions (10). These and related considerations suggest that Eq. 6 tends to underestimate $\Delta G^*(int)$ (10); on the other hand, deviations in the opposite direction are suggested from a molecular dynamics solvent model (11).

In the following sections, some recent experimental data gathered in our laboratory that provide illustrative examples of these solvent effects will be presented. For brevity, experimental and related details are omitted; these can be found in the articles cited.

II. Interfacial Solvation Effects - Variation of Solvent

Several sets of measurements will be described that provide evidence for the influence of interfacial solvation to the electrode kinetics of simple inorganic redox couples. The first involve the comparison between the solvent dependence of standard rate constants, k_{corr}^s , for $Ru(NH_3)_6^{3+/2+}$ and $Co(en)_3^{3+/2+}$ (en = ethylenediamine) at mercury electrodes with the corresponding values, k_{calc}^s , calculated from theoretical models on the basis of Eq. 5. Details of the latter calculations are given in refs. 12 and 13. Values of $\Delta G_s^*(int)$ were obtained from vibrational and bond length data (13), the solvent-dependent $\Delta G_{os}^*(int)$ values were obtained from Eq. 6 with $a = 3.5$ Å, $R = 14$ Å in water, and $R = 17$ Å in nonaqueous media (12). The value of v_n is equated with v_{is} (*vide infra*), 1×10^{13} sec⁻¹ for both couples (13); K_o is taken as 0.6 Å, Γ_n equals 1.05 and 3.0 for $Ru(NH_3)_6^{3+/2+}$ and $Co(en)_3^{3+/2+}$ in various solvents, taken from refs. 6, 12, 14, and 15, are listed in Table I. Whereas small increases in k_{calc}^s are predicted upon substitution of aqueous by nonaqueous (particularly aprotic) media, large (up to 10^3 fold) decreases

TABLE I Solvent Dependence of Standard Rate Constants for $\text{Ru}(\text{NH}_3)_6^{3+/2+}$ and $\text{Co}(\text{en})_3^{3+/2+}$ (en = ethylenediamine) at Mercury Electrodes

Redox Couple	Solvent ^a	A_{corr}^b cm sec ⁻¹	k_{corr}^c cm sec ⁻¹	k_{calc}^d cm sec ⁻¹	DN ^e
$\text{Ru}(\text{NH}_3)_6^{3+/2+}$	H ₂ O	5×10^3	2.0	2.5	~18
	PC		~3	5	15.1
	DMF	25	0.25	10	26.6
	DMSO	2.5×10^2	5×10^{-2}	15	29.8
$\text{Co}(\text{en})_3^{3+/2+}$	H ₂ O	0.7	2.5×10^{-2}	3×10^{-4}	~18
	F	8×10^5	1.5×10^{-3}	7×10^{-4}	~24
	NMF	2×10^6	6×10^{-4}	7×10^{-4}	27
	PC		3×10^{-4}	7×10^{-4}	15.1
	AN	2×10^5	1.5×10^{-3}	5×10^{-4}	14.1
	DMF	2.5×10^6	1×10^{-5}	1.2×10^{-3}	26.6
	DMSO	1×10^7	1×10^{-5}	2×10^{-3}	29.8

^aPC = propylene carbonate, DMF = N,N-dimethylformamide, DMSO = dimethylsulfoxide, F = formamide, NMF = N-methylformamide, AN = acetonitrile

^bDouble-layer corrected preexponential factor, obtained from intercept of Arrhenius plot of $\ln k_{\text{corr}}^s$ versus (1/T) (see text).

^cDouble layer-corrected standard rate constant, obtained from observed rate constant (measured using either a.c. or normal pulse polarography), by using Eq. 4.

^dCalculated standard rate constant, obtained as described in text.

^eSolvent "donor number", from ref. 16.

in k_{corr}^s are obtained instead. This marked solvent dependence of k_{corr}^s for $\text{Co}(\text{en})_3^{3+/2+}$ has previously been ascribed tentatively to increases in $\Delta G_{\text{os}}^*(\text{int})$ associated with specific ligand-solvent interactions, perhaps with accompanying decreases in κ_{el} (6). This explanation is consistent with the observation that k_{ob}^s decreases with increasing ligand-solvent interactions as monitored by the solvent donor number (Table I) (6,7).

However, several pieces of additional information suggest that the substantial solvent dependences of k_{corr}^s for both $\text{Co}(\text{en})_3^{3+/2+}$ and $\text{Ru}(\text{NH})_6^{3+/2+}$ are due primarily to variations in K_0 associated with differences in reactant solvation in the bulk and interfacial environments. In particular, we have found that sufficiently high two-dimensional concentrations (ca $1-5 \times 10^{-11}$ mol cm^{-2}) of $\text{Co}(\text{en})_3^{3+}$, $\text{Co}(\text{NH}_3)_6^{3+}$ and certain other ammine complexes can be induced via electrostatic attraction at the silver-aqueous interface containing adsorbed chloride or bromide anions so to enable their reduction kinetics to be monitored directly in the precursor state at the outer Helmholtz plane by means of rapid linear sweep voltammetry (18). (Indeed, such diffuse-layer cations also exhibit detectable surface-enhanced Raman spectra (19).) These measurements enable *unimolecular* rate constants for the elementary electron-transfer step, k_{et} , to be evaluated. (This is directly analogous to the measurement of k_{et} for outer-sphere cation-anion pairs in homogeneous solution (20).) After a correction for electrostatic double-layer effects, comparison of the resulting k_{et} values with k_{corr} for the same reaction obtained at the mercury-aqueous interface at the same electrode potential enables K_0 for the latter to be estimated since (1)

$$k_{\text{corr}} = K_0 k_{\text{et}} \quad \text{Eq. 7}$$

The resulting estimates of K_0 for $\text{Co}(\text{en})_3^{3+/2+}$ and $\text{Co}(\text{NH}_3)_6^{3+}$, ca 200 and 10 Å, respectively, are markedly larger than the value of 0.6 Å, anticipated for weakly adiabatic processes (1,13), that was assumed when deriving the k_{calc} values in Table I. A similarly large estimate of K_0 , ca 5 Å, has been obtained for reduction of Cr(III) amines at the mercury-aqueous interface by using a related procedure whereby k_{corr} for the outer-sphere reaction is compared with k_{et} for a structurally related inner-sphere reaction (21). The same procedure yields a substantially smaller reaction zone thickness, ca 0.1 - 0.3 Å, for Cr(III) aquo reductions (21).

These results suggest that unexpectedly high concentrations of ethylenediamine and ammine reactants are present at mercury-aqueous interfaces, most likely associated with differences in the outer-shell solvation of the reactant in the bulk and

interfacial environments, and possibly to partial reactant desolvation at the electrode surface. This is consistent with the data in Table I in that such surface environmental effects are less likely in nonaqueous solvents having high donor numbers than in aqueous media. Therefore "normal" outer-sphere pathways, associated with smaller values of K_o and hence k_{corr}^s , are expected in the former solvents. The general observation that $k_{\text{corr}}^s < k_{\text{calc}}^s$ in aprotic media (Table I) may be due to several factors, including the occurrence of nonadiabatic pathways (i.e., $\kappa_{el} < 1$) as well as to outer-shell barriers that are larger than estimated using the dielectric continuum model.

Of interest in this regard are the experimental frequency factors, A_{corr} (cm sec^{-1}), also listed in Table I. These were obtained from the temperature dependence of k_{corr}^s by using

$$\ln A_{\text{corr}} = \ln k_{\text{corr}} - (1/T)[d \ln k_{\text{corr}} / d(1/T)] \quad \text{Eq. 8}$$

To a first approximation A_{corr} can be identified with the combined preexponential factor in Eq. 5, $K_o \nu_n \kappa_{el} \Gamma_n$, provided that these terms are temperature independent. For the present systems, it is expected that $A_{\text{corr}} \approx 10^4$ - 10^5 cm sec^{-1} . The abnormally small value of A_{corr} , 0.7 cm sec^{-1} , for $\text{Co(en)}_3^{3+/2+}$ in water (Table I) is further evidence of the deviation of this reaction from a "normal" outer-sphere pathway. The much larger A_{corr} values (10^5 - 10^7 cm sec^{-1}) seen for $\text{Co(en)}_3^{3+/2+}$ in nonaqueous media (Table I) are closer to the theoretical expectations and indicate that the correspondingly smaller values of k_{corr}^s are unlikely to be due to decreases in κ_{el} .

III. Interfacial Solvation Effects - Alteration of Electrode Material

As noted above, in principle an interesting way of varying the interfacial solvent environment while maintaining other factors, including bulk solvation, constant is to alter the chemical nature of the metal surface (22). Given the complex hydrogen-bonded nature of liquid water, marked changes in its structure are anticipated even over several molecular layers near surfaces known to interact specifically with water (i.e., "hydrophilic surfaces") (23). It is therefore of interest to examine outer-sphere rate data at surfaces of differing hydrophilicity. One difficulty with interpreting rate constants as a function of the electrode material is the uncertainties in the electrostatic double-layer corrections, especially at polycrystalline solid surfaces and in the presence of extensive specific adsorption of the supporting electrolyte. The results of some recent experiments designed to minimize these

difficulties (24) will now be briefly described.

Table II contains representative electrochemical rate data for the irreversible reduction of four Cr(III) complexes at five metal surfaces in contact with aqueous solution. These reactions are all irreversible; a common potential of -1000 mV vs. saturated calomel electrode (s.c.e.) was chosen to facilitate intercomparison of the data. This potential is sufficiently negative so to essentially eliminate specific anion adsorption with the perchlorate or hexafluorophosphate electrolytes employed. The five metal surfaces; liquid mercury and gallium, lead, and underpotential deposited (upd) monolayers of lead and thallium at silver, all provide relatively well-defined electrodes yet with significant anticipated differences in their hydrophilicity (25).

The observed rate constants for each reaction in Table II vary substantially as the electrode material is altered. Part of these variations are undoubtedly due to electrostatic double-layer effects since the metals yielding smaller k_{ob} values also exhibit the most negative potentials of zero charge (p.z.c.) where ϕ_r will be the least negative [Eq. 4]. However, the corresponding k_{corr} values listed in Table II, obtained by applying Eq. 4 (24) also exhibit similar dependencies on the metal substrate as for the aquo reactants. This correction yields roughly substrate-independent values of k_{corr} for $Cr(NH_3)_6^{3+}$ reduction. Support for the validity of these double-layer corrections is provided by the similar substrate dependencies of k_{corr} for all three aquo complexes, even though the corrections are smaller for the fluoro and especially the sulfato complex on account of their smaller net cationic charge (26). The relative magnitudes of k_{corr} for each complex are also virtually independent of the electrode potential since the work-corrected transfer coefficients, α_{corr} , are also almost independent of the metal surface. Comparable results have also been observed for several other reactions involving aquo and ammine complexes (24).

Significantly, the observed dependence of k_{corr} for the aquo complexes on the metal surface, $Hg > upd Pb \sim upd Tl \geq Pb > Ga$ is consistent with the anticipated differences in their hydrophilities (24). The disparate behavior of mercury and gallium is particularly interesting since these both provide well-defined liquid surfaces; the former has only a small, and the latter a large, tendency to bind to the oxygen atom of water (25). The most likely, albeit not the sole, possibility is that K_o and/or κ_{el} for the aquo complex reductions are decreased substantially (up to ca 10^3 -fold) upon substituting more hydrophilic surfaces for mercury. This observed sensitivity of the aquo complexes to the surface environment, and the relative lack of such an

10

TABLE II Rate Constants for the Electroreduction of Cr(III) Complexes at -1000 mV vs s.c.e. at Various Metal Surfaces at 25°C

Reactant	Surface	k_{ob}^a cm sec ⁻¹	α_{ob}^b	k_{corr}^c cm sec ⁻¹	α_{corr}^d
$Cr(OH_2)_6^{3+}$	Hg	5×10^{-2}	0.61	3×10^{-3}	0.50
	Ga	8×10^{-6}	0.58	3×10^{-6}	0.50
	Pb	3×10^{-5}	0.61	1.5×10^{-5}	0.55
	upd Pb	3×10^{-3}	0.55	1.5×10^{-3}	0.52
	upd Tl	3×10^{-4}	0.50	3×10^{-4}	0.50
$Cr(OH_2)_5F^{2+}$	Hg	2.5×10^{-4}	0.58	2.5×10^{-5}	0.54
	Pb	2×10^{-6}	0.55	1×10^{-6}	0.52
	upd Pb	$\sim 2 \times 10^{-5}$	0.55	$\sim 1 \times 10^{-5}$	~ 0.55
	upd Tl	1.5×10^{-6}	0.65	1.0×10^{-6}	0.6
$Cr(OH_2)_5OSO_3^+$	Hg	3.5×10^{-3}	0.54	2×10^{-3}	0.52
	Ga	$\sim 7 \times 10^{-6}$	~ 0.55	$\sim 5 \times 10^{-6}$	~ 0.55
	Pb	3×10^{-5}	0.5	2.5×10^{-5}	~ 0.5
	upd Pb	5×10^{-5}	0.5	3×10^{-5}	~ 0.5
$Cr(NH_3)_6^{3+}$	Hg	2×10^{-2}	0.84	4×10^{-4}	0.75
	Ga	$\sim 2 \times 10^{-4}$	0.8	1.5×10^{-4}	~ 0.7
	Pb	6×10^{-6}	0.76	1.5×10^{-6}	0.7
	upd Pb	2.5×10^{-4}	0.78	7×10^{-5}	0.70
	upd Tl	8×10^{-5}	0.70	7×10^{-5}	0.65

^a Observed rate constant for one-electron electroreduction of complex at electrode potential $E = -1000$ mV at metal surface listed; electrolyte was $0.5 \text{ M NaClO}_4 + 3 \text{ mM HClO}_4$, except for $Cr(NH_3)_6^{3+}$ reduction which was measured in $40 \text{ mM La(ClO}_4)_3 + 3 \text{ mM HClO}_4$.

^b Observed transfer coefficient, determined from $\alpha_{ob} = -(RT/F)(d \ln k_{ob}/dE)$.

^c Rate constant at -1000 mV corrected for electrostatic work terms, determined from listed value of k_{ob} using Eq. 4; required values of the diffuse-layer potential ϕ_r determined as noted in ref. 24.

^d Transfer coefficient corrected for electrostatic work terms (24).

11

effect for $\text{Cr}(\text{NH}_3)_6^{3+}$ reduction, may well be associated with the especially strong hydrogen bonding between aquo ligands and surrounding water molecules (27). Approach of such aquo reactants to hydrophilic metal surfaces may necessitate disturbance of this secondary solvation since the electrode will tend to orient water molecules so to impede solvation of nearby reactant cations.

The likelihood that the hydrophilic surfaces induce substantial perturbations upon the interfacial reactant solvation is supported by the decreases in the activation enthalpies, ΔH^\ddagger , that accompanying decreases in k_{corr} (24). Moreover, the observed rate constants and activation parameters for $\text{Cr}(\text{OH}_2)_6^{3+}$ reduction at mercury electrodes are substantially closer to the numerical predictions obtained from the above rate formalisms than those observed at the hydrophilic surfaces (12,24). This further indicates that the mercury surface provides an relatively "nonperturbing" environment for aquo reactants. The distinctly different behavior exhibited by reactions involving otherwise-similar aquo and ammine (and ethylenediamine) reactants is broadly speaking consistent with the distinctly weaker hydration of the latter. The former can usefully be regarded as "surface-structure sensitive" processes, associated with strong aquo ligand-solvent interactions. The weaker solvent interactions experienced by the ammine reactants lead to substantial deviations from "normal" outer-sphere behavior at the weakly solvated mercury surface, which nonetheless appear to be relatively insensitive to the surface hydrophilicity.

Another series of systems that illustrate the ligand-dependent influences of interfacial solvation upon electrochemical kinetics at the mercury-aqueous interface is provided by examinations of the electroreduction kinetics of $\text{Co}^{\text{III}}(\text{NH}_3)_5\text{L}^{2+}$ complexes, where L is a carboxylate ligand containing a variety of organic substituents that nonetheless lack a surface binding group (28). Large (up to 10^4 -fold) variations in k_{corr} at a given electrode potential are observed as L is varied, even though similar reactivities are observed for the homogeneous reduction of all these complexes by the outer-sphere reductant $\text{Ru}(\text{NH}_3)_6^{2+}$ (28). Generally, k_{corr} increases as the "hydrophobic" nature of L is increased, especially when L contains one or more aromatic rings, suggesting that the cross-sectional reactant concentration at the interface, and hence K_0 , increases as the strength of reactant-solvent interactions decreases. On the other hand, closely similar values of k_{corr} are observed for all these reactions at the mercury-dimethylsulfoxide interface. This again demonstrates the predominance of "normal" outer-sphere pathways, at least for cationic reactants, in this more strongly solvating medium.

Regardless of the physical details, it seems clear that the nature of the interfacial environment can yield significant and even substantial influences upon the reaction energetics of ostensibly outer-sphere electrode reactions in aqueous solution. Generally speaking, large deviations from the reactivities expected for normal outer-sphere pathways occur when the reactant-solvent interactions are relatively weak, even for reactants not expected to replace the inner-layer solvent molecules. This circumstance may encompass the large majority of electrode reactions involving cationic inorganic reactants in aqueous solution, as well as for anionic species which often proceed via adsorbed transition states under these conditions.

IV. Solvent Relaxation Dynamics

As is conventional, we have assumed so far that the frequency factor of the electron-transfer step is independent of the surrounding solvent. On the basis of the encounter pre-equilibrium formulation [Eqs. 1 or 5], the frequency for adiabatic pathways ($\kappa_{el} \sim 1$) is identified with ν_n . On the basis of the transition-state treatment (TST), ν_n can be expressed as a weighted mean of the characteristic inner-shell and outer-shell (solvent) frequencies, ν_{is} and ν_{os} , as (1,29)

$$\nu_n = \left(\frac{\nu_{os}^2 \Delta G_{os}^* + \nu_{is}^2 \Delta G_{is}^*}{\Delta G_{os}^* + \Delta G_{is}^*} \right)^{1/2} \quad \text{Eq. 9}$$

Since it is commonly presumed that $\nu_{os} \ll \nu_{is}$, even when $\Delta G_{is}^* < \Delta G_{os}^*$, the overall frequency factor is anticipated to commonly be dominated by ν_{is} rather than by ν_{os} . Recent theoretical treatments, however, suggest instead that the dynamics of solvent reorganization may play an important role in the kinetics of outer-sphere electron-transfer reactions, at least when the inner-shell barrier is small (30,31). We now briefly summarize the resulting relationships, and utilize them to examine the solvent-dependent electrochemical exchange kinetics for some metallocene redox couples.

It has been pointed out that the effective value of ν_{os} can often be determined by the so-called longitudinal (or "constant charge") solvent relaxation time, τ_L (30,31). This quantity is related to the experimental Debye relaxation time, τ_D , obtained from dielectric loss measurements using

$$\tau_L = (\epsilon_\infty / \epsilon_s) \tau_D \quad \text{Eq. 10}$$

where ϵ_∞ is the high-frequency solvent dielectric constant. For solvents where $\tau_L \geq 10^{-12}$ sec⁻¹, ν_{os} is dominated by the solvent relaxation frequency, ν_{os}^L , such that for electron-exchange reactions (i.e., when the free-energy driving force is zero) (30,31):

$$\nu_{os}^L = \tau_L^{-1} \left(\frac{\Delta G_{os}^*}{4\pi k_B T} \right)^{1/2} \quad \text{Eq. 11}$$

where k_B is the Boltzmann constant. Since τ_L typically falls in the range ca 10^{-11} to 2×10^{-13} sec for common electrochemical solvents (32), when $\Delta G_{os}^* \sim 5$ kcal mol⁻¹ ν_{os}^L will lie in the range ca 10^{11} to 3×10^{12} sec⁻¹. Since ν_{is} for systems involving metal-ligand vibrations will typically be close to 1×10^{13} sec⁻¹, generally $\nu_{os}^L < \nu_{is}$. It is important to note, however, that in contrast to Eq. 9 which refers to the rate of barrier crossing, Eq. 11 describes deviations from TST where ν_{os} is controlled by the rate of *approaching* the barrier top associated with slow solvent relaxation. Consequently, ν_{os}^L will tend to dominate ν_n when $\nu_{os}^L \ll \nu_{is}$; i.e. the *slowest* activation mode controls the effective frequency factor. This is the opposite result to that anticipated from TST (33). For rapidly relaxing solvents, when $\nu_{os}^L \leq 10^{-12}$ sec⁻¹, the effective outer-shell frequency can be controlled partly by solvent rotation, i.e., "solvent inertial" effects (30). Approximate expressions are available with which to estimate this frequency, ν_{os}^R , which corresponds to the TST limit (30).

Similarly to the TST limit, the relative contributions of ν_{os}^L and ν_{is} to ν_n will be weighted according to the relative magnitudes of ΔG_{os}^* and ΔG_{is}^* to the overall barrier height, although Eq. 9 is no longer appropriate. The circumstance $\nu_{os}^L = \nu_n$ is anticipated to hold for exchange reactions when approximately (34)

$$(\Delta G_{is}^* / \Delta G_{int}^*)^{1/2} \nu_{is} \exp(-\Delta G_{is}^* / k_B T) \geq \tau_L^{-1} \quad \text{Eq. 12}$$

For the typical values $\Delta G_{int}^* = 5$ kcal mol⁻¹, $\nu_{is} = 1 \times 10^{13}$ sec⁻¹, $\tau_L \leq 5 \times 10^{-12}$ sec, this inequality will hold when $\Delta G_{is}^* \leq 1$ kcal mol⁻¹. This last condition is expected to be the case for a variety of redox couples where the bond distortions required for electron transfer are relatively small (e.g., aromatic molecule-anion, transition-metal couples containing aromatic ligands). We therefore expect that for such "rapid" electron-exchange systems the effective frequency factor will be determined by solvent reorientation.

Since τ_L and hence ν_{os}^L can vary greatly (ca 50 fold) with the solvent size and intermolecular structure, this circumstance

can provide a large and even dominant influence on the solvent dependence of k_{corr} . We have evaluated standard electrochemical rate constants as a function of solvent at mercury electrodes for several cationic metallocene couples having the general form $M(\text{Cp})_2^{+/0}$ or $M(\text{Cp}')_2^{+/0}$, where $M = \text{Fe, Mn, Co}$, $\text{Cp} = \text{cyclopentadienyl}$, and $\text{Cp}' = \text{pentamethylcyclopentadienyl}$ (32,35). These couples have several important virtues for such fundamental examinations of solvent effects. In particular, only small changes ($\leq 0.04 \text{ \AA}$) in the metal-ring bond distances accompany electron transfer (36); together with corresponding Raman vibrational data these yield small yet varying inner-shell barriers, ΔG_{is}^* (int) ~ 0.025 to $0.25 \text{ kcal mol}^{-1}$. Nevertheless, the relatively small size of the complexes ($a = 3.5 - 4 \text{ \AA}$) yields sufficiently large ΔG_{os}^* (int) values so that the k_{ob}^{S} values are conveniently measureable (ca $0.1 - 2 \text{ cm sec}^{-1}$) using a.c. polarography. In addition, the formal potentials E_f can be varied between 0 and -1.5 V vs s.c.e. by altering the metal and substituting methyl groups on the cyclopentadienyl rings. The magnitude of the electrostatic double-layer corrections appears to be small under most conditions, so that $k_{\text{ob}}^{\text{S}} = k_{\text{corr}}^{\text{S}}$ (35).

Table III contains values of k_{ob}^{S} for two representative metallocene couples, $\text{Fe}(\text{Cp}')_2^{+/0}$ and $\text{Co}(\text{Cp})_2^{+/0}$, together with data for the closely related dibenzenechromium couple, $\text{Cr}(\text{C}_6\text{H}_6)_2^{+/0}$ in eight nonaqueous solvents; acetonitrile (ACN), acetone, methylene chloride (CH_2Cl_2), formamide, N-methylformamide (NMF), N,N-dimethylformamide (DMF), dimethylsulfoxide (DMSO) and benzonitrile ($\text{C}_6\text{H}_5\text{CN}$). These solvents were chosen not only for their suitability for electrochemical measurements but also because of the wide variations between the values of τ_L , and hence v_{os}^{L} obtained from Eqs. 10 and 11. These v_{os}^{L} values vary from $4.5 \times 10^{12} \text{ sec}^{-1}$ in acetonitrile to $1.3 \times 10^{11} \text{ sec}^{-1}$ in benzonitrile.

To the left of the experimental k_{ob}^{S} values are listed two sets of calculated rate constants, $k_{\text{calc}}^{\text{S}}$. The first set, labelled "Eq. 9", were obtained using Eq. 5 by calculating v_n from Eq. 9, assuming that $v_{\text{is}} \gg v_{\text{os}}$, and ΔG_{is}^* (int) = $0.2 \text{ kcal mol}^{-1}$ (a typical value for the reactants considered here (32,35)). (Other calculational details are given in the footnotes to Table III and in refs. 32 and 35.) Since the frequency factor using this approach will be solvent independent, the resulting solvent dependence of $k_{\text{calc}}^{\text{S}}$ arises entirely from the predicted variations in the outer-shell barrier, ΔG_{os}^* (int), obtained from Eq. 6. Comparison between the values of k_{ob}^{S} and $k_{\text{calc}}^{\text{S}}$ (Eq. 9) shows that whereas rough agreement is seen in some solvents, the latter entirely fail to account for the observed solvent dependence of k_{ob}^{S} , the ca 13-fold increase in $k_{\text{calc}}^{\text{S}}$ from acetonitrile to benzonitrile contrasting the observed ca 3-5 fold decreases in k_{ob}^{S} .

TABLE III Comparison between Calculated and Experimental Rate Constants (cm sec^{-1}) for Electrochemical Exchange at Mercury-Nonaqueous Interfaces at 23°C

Solvent	Calculated Rate Constants, k_{calc}^s (Eq. 9) ^a , k_{calc}^s (Eq. 11) ^b		Observed Rate Constants, k_{ob}^s ^c		
			$\text{Fe}(\text{Cp}')^{+/-}_2$	$\text{Co}(\text{Cp})^{+/-}_2$	$\text{Cr}(\text{C}_6\text{H}_6)_2^{+/-}$
ACN	0.30	1.6		1.0	1.8
Acetone	0.55	2.0	2.2	0.95	1.2
CH_2Cl_2	4.0	10	0.45	0.25	0.45
Formamide	0.9	0.38		0.19	0.17
NMF	0.7	0.20	0.45	0.32	0.40
DMF	1.0	0.60	0.8	0.38	0.55
DMSO	2.5	0.7	0.25	0.15	0.11
$\text{C}_6\text{H}_5\text{CN}$	4.2	0.65	0.45	0.32	0.3

^aStandard rate constant (cm sec^{-1}) calculated from Eq. 5, with $\Delta G_{\text{is}}^{\ddagger}(\text{int}) = 0$, $\Delta G_{\text{os}}^{\ddagger}(\text{int})$ from Eq. 6 with $a = 3.8 \text{ \AA}$, $R = \infty$, $\Gamma = 1$, $K_{\text{ocel}} = 0.6 \text{ \AA}$, v_n obtained from Eq. 9, with $\Delta G_{\text{is}}^{\ddagger}(\text{int}) = 0.2 \text{ kcal mol}^{-1}$, $v_{\text{is}} = 6 \times 10^{12} \text{ sec}^{-1}$, and $v_{\text{os}} \ll v_{\text{is}}$ (see text).

^bAs footnote a, but with v_n set equal to v_{os}^L obtained from Eq. 11 using literature dielectric loss data (see refs. 32,35).

^cObserved rate constant (cm sec^{-1}) obtained for stated redox couple in solvent indicated, containing 0.1 M TBAP. Cp = cyclopentadienyl; Cp' = pentamethylcyclopentadienyl.

The second set of k_{calc}^s values in Table III, labelled "Eq. 11" were obtained using the same procedure as the first set, but with v_n estimated instead by equating it with v_{os}^L obtained from Eq. 11. [This condition $v_n = v_{\text{os}}^L$ is predicted for the present systems from Eq. 12.] In contrast to k_{calc}^s (Eq 9), these latter calculated values not only approximate the k_{ob}^s values in most solvents, but also correctly mimic the observed solvent dependence of k_{ob}^s (the sole exception is the data in methylene chloride). Such reasonable agreement between experiment and the theoretical predictions also extends to the electrochemical activation parameters (35).

It is interesting to note that, broadly speaking, as ϵ_{op} increases [and hence $\Delta G_{\text{os}}^{\ddagger}(\text{int})$ decreases] in a series of solvents (such as those in Table III), τ_L^{-1} and hence v_{os}^L tend to decrease. Consequently, the solvent dependence of the free-energy barrier and relaxation dynamics associated with outer-shell reorganization tend to offset each other. This circumstance can account both for the otherwise-perplexing solvent independence of exchange

kinetics for some systems (37) as well as solvent-dependent rate ratios that are opposite from the expectations of the conventional theoretical treatment. (For example, values of k_{ob}^s in acetonitrile are often observed to be larger than in DMF, despite the greater values of $\Delta G_{os}^*(int)$ in the former solvent.) Most importantly, the present evidence suggests that the dielectric continuum model can provide a reasonable representation of the reaction energetics, at least for reactants (such as metallocenes) that interact nonspecifically with the surrounding solvent, providing that the role of the solvent in the preexponential as well as the exponential factor (free-energy barrier) is taken into account. Nevertheless, according to Eq. 12 the former should be limited to reactants having relatively small inner-shell barriers. If feasible, it would be most interesting to examine solvent-dependent exchange kinetics for a series of structurally related redox couples having inner-shell barriers that could be varied over the range, say, from zero to 2 kcal mol⁻¹ where the circumstance $v_n = v_{os}$ should give way to $v_n = v_{is}$.

V. Concluding Remarks

The foregoing provides several lines of evidence that indicate that the chemical nature of the solvent can yield important influences on electron-transfer kinetics even for outer-sphere electrochemical reactions where the inner-shell barrier is held constant. Several other types of experiments, for example those involving mixed solvents with preferential solvation of the surface and/or the reacting species, also lead to the same general conclusions. The theoretical formalisms utilized here, especially the dielectric continuum solvent model, should be used with caution in view of the simplifying assumptions involved. Nonetheless, the observed large sensitivities of the electrochemical rate data to the solvent medium can be satisfyingly rationalized, at least semiquantitatively, in terms of these models.

As noted at the outset, our fundamental understanding of solvent effects in electrochemical and other electron-transfer reactions remains rudimentary. However, the renaissance of theoretical activity in condensed-phase reaction dynamics (38) together with further critical experimental work should provide fresh insight into the role of the solvating environment for electron-transfer reactions in the near future.

Acknowledgments

Dr. Joseph Hupp contributed importantly to several facets of the present work. Prof. J. T. Hynes provided some valuable insights into solvent dynamics. This work is supported in part by the Office of Naval Research and the Air Force Office of Scientific Research. The author acknowledges a fellowship from the Alfred P. Sloan Foundation.

References

1. J. T. Hupp, M. J. Weaver, J. Electroanal. Chem. 152, 1 (1983).
2. J. T. Hupp, M. J. Weaver, J. Phys. Chem. 88, 1463 (1984).
3. P. Delahay, "Double Layer and Electrode Kinetics", Interscience, New York, 1965, Chapter 9.
4. For example, J. Logan, M. D. Newton, J. Chem. Phys. 78(2), 4086 (1983).
5. R. A. Marcus, J. Phys. Chem. 72, 891 (1968).
6. S. Sahami, M. J. Weaver, J. Electroanal. Chem. 124, 35 (1981).
7. R. A. Marcus, J. Chem. Phys. 43, 679 (1965).
8. For example, J. O'M. Bockris, S. V. M. Khan, "Quantum Electrochemistry", Plenum Press, New York, 1979.
9. C. Creutz, Prog. Inorg. Chem. 30, 1 (1983); T. J. Meyer, *ibid* 30, 389 (1983).
10. J. T. Hupp, M. J. Weaver, submitted for publication; J. T. Hupp, M. J. Weaver, J. Phys. Chem. 88, 1860 (1984).
11. D. F. Calef, P. G. Wolynes, J. Chem. Phys. 78, 470 (1983).
12. J. T. Hupp, H. Y. Liu, J. K. Farmer, T. Gennett, M. J. Weaver, J. Electroanal. Chem., in press.
13. J. T. Hupp, M. J. Weaver, submitted.
14. J. K. Farmer, J. T. Hupp, T. Gennett, M. J. Weaver, in preparation.
15. T. Gennett, M. J. Weaver, Anal. Chem., in press.

16. V. Gutmann, "The Donor-Acceptor Approach to Molecular Interactions", Plenum Press, New York, 1978, Chapter 2.
17. S. Sahami, M. J. Weaver, J. Electroanal. Chem. 122, 171 (1981).
18. M. A. Tadayyoni, M. J. Weaver, to be published.
19. M. A. Tadayyoni, S. Farquharson, M. J. Weaver, J. Chem. Phys. 80, 1363 (1984).
20. D. Gaswick, A. Haim, J. Am. Chem. Soc. 93, 7347 (1971).
21. J. T. Hupp, M. J. Weaver, J. Phys. Chem. 88, 1463 (1984).
22. S. Trassati, in "Advances in Electrochemistry and Electrochemical Engineering", H. Gerischer, C. W. Tobias (eds), Wiley, New York, Vol. X, 1977, p. 279.
23. W. Drost-Hansen, Ind. Eng. Chem. 61 (11), 10 (1969).
24. H. Y. Liu, J. T. Hupp, M. J. Weaver, J. Electroanal. Chem., in press.
25. S. Trassati, in "Modern Aspects of Electrochemistry", Vol. 13, B. E. Conway, J. O'M. Bockris (eds), Plenum, New York, 1979, p. 81; S. Trassati, Electrochim. Acta 28, 1083 (1983).
26. M. J. Weaver, F. C. Anson, Inorg. Chem. 15, 1871 (1976); J. Phys. Chem. 80, 1861 (1976).
27. E. L. Yee, R. S. Cave, K. L. Guyer, P. D. Tyma, M. J. Weaver, J. Am. Chem. Soc. 101, 1131 (1979); M. J. Weaver, S. M. Nettles, Inorg. Chem. 19, 1641 (1980).
28. V. Srinivansan, S. W. Barr, M. J. Weaver, Inorg. Chem. 21, 3154 (1982); T. T-T. Li, M. J. Weaver, in preparation.
29. N. Sutin, Prog. Inorg. Chem. 30, 441 (1983).
30. D. F. Calef, P. G. Wolynes, J. Phys. Chem. 87, 3387 (1983).
31. L. D. Zusman, Chem. Phys. 49, 295 (1980); I. V. Alexandrov, Chem. Phys. 51, 449 (1980).
32. M. J. Weaver, T. Gennett, Chem. Phys. Lett., submitted.
33. B. L. Tembe, H. L. Friedman, M. D. Newton, J. Chem. Phys. 76, 1490 (1982).

34. M. Ya Ovchinnikova, Russ. Theor. Exp. Chem. 17, 507 (1981).
35. T. Gennett, H. J. Weaver, submitted.
36. A. Hazland, Acc. Chem. Res. 12, 415 (1979).
37. E. S. Yang, M-S. Chan, A. C. Wahl, J. Phys. Chem. 84, 3094 (1980).
38. For example, see D. G. Truhlar, W. L. Hase, J. T. Hynes, J. Phys. Chem. 87, 2664 (1983).

END

FILMED

10-84

DTIC